Electronic Supplementary Information

Boosting the chemoselective production of biomass-derived butanediol by bifunctional Pd-WO_x catalysts modified with MgO_y species

Heng Huang[ab], Haijie Yu[ab], Jiayi Peng[b], Yueyue Tang[b], Renhui Ling[b], Jianjian Wang[ab*]

[a] School of Chemistry and Chemical Engineering, Institute of Advanced Interdisciplinary Studies, Multi-scale Porous Materials Center, Chongqing University, Chongqing, 401331, China.

[b] State Key Laboratory of Coal Mine Disaster Dynamics and Control, Chongqing University, Chongqing, 401331, China.

* Corresponding author: wangjianjian@cqu.edu.cn.

Experimental Section

Materials

$PdCl_2$ (99%), WCl_6 (99%), ethylene glycol (EG, 98%), 1,2-propanediol (1,2-PDO, 99%), 1,3-propanediol (1,3-PDO, 98%), 1,2-butanediol (1,2-BDO, >98%), 1,4-butanediol (1,4-BDO, 99%), glucose (99%), pyridine (>99%), $Mg(NO_3)_2{\cdot}6H_2O$ (AR, 99%), $Zr(NO_3)_4{\cdot}5H_2O$ (AR,99%), $Al_2(NO_3)_3{\cdot}9H_2O$ (AR,99%), and $Cr_2(NO_3)_3{\cdot}9H_2O$ were purchased from Aladdin Company. Ethanol (>99%) was purchased from KESHI Company. All chemicals were directly used without further purification.

Characterization

Powder X-ray diffraction (XRD) pattern was recorded on a PANalytical apparatus with a Cu Kα radiation (λ = 0.1542 nm) in the range of 5-80° at a speed of 5° min^{-1}. Fourier transform infrared spectroscopy (FTIR) was performed on a NICOLET iS50 instrument. Thermogravimetric analysis (TGA) was conducted on a TGA2 from Mettler Toledo Company in the air of catalysts, measuring temperature from 30 °C to 800 °C. Inductively coupled plasma optical emission spectrometer (ICP-OES) was performed on VARIAN 710-ES. Solid samples were dissolved in nitric acid and diluted before measurement. Nitrogen adsorption and desorption isotherms of the samples were measured at 77 K with a BELSORP MAX apparatus from MicrotracBEL company. BET surface areas were calculated using the desorption isotherms. All samples were outgassed at 160 °C for 12 h before measurement. Hydrogen temperature-programmed reduction (H_2-TPR) and hydrogen temperature-

programmed (H_2-TPD) desorption were performed on a MICROTRAC BELCAT apparatus. Approximately 50 mg of each sample was placed in quartz reactors and reduced in a stream of 50 mL min^{-1} 10% H_2/Ar at a heating rate of 10 °C min^{-1}. NH_3 temperature-programmed desorption with both thermal conductivity detector (TCD) and mass spectrometer (MS) detectors was performed on a BSD-C200 apparatus. About 100 mg of the sample was pretreated in a He atmosphere at 300 °C for 1 h; after subsequent cooling to 50 °C, 10% NH_3/He mixture flowing gas (30−50 mL min^{-1}) was introduced for 1 h until adsorption saturation. The tube was purged with a pure He flow for 1 h to remove the weak physical adsorption of NH_3 on the surface. The sample was desorbed and heated to 800 °C at a rate of 10 °C min^{-1} in a He atmosphere with a record of TCD. X-Ray Photoelectron Spectroscopy (XPS) was conducted on a Thermo Scientiffc K-Alpha. The binding energy values (B.E.) were estimated after positioning the C 1s peak of the contaminant carbon at 284.8 eV. Transmission electron microscopy (TEM) and energy-dispersive X-ray spectroscopy (EDS) mapping were conducted on a FEI Talos 200S with an operating voltage of 200 kV. In situ diffuse reflectance infrared Fourier transform spectroscopy (DRIFTS) was conducted on a SHIMADZU IRTracer-100 equipped with a MCT detector The sample amount loaded in the DRIFTS cell (HARRICK) was around 50 mg and the gas flow rate was kept at 20 mL/min. Using a blank catalyst as the background, maintain the sample at different test temperatures for 0.5 hours and collect infrared spectra.

Catalytic evaluation

Typically, experiment for catalytic conversion of biomass was performed in a 25 mL autoclavable reactor. Each experiment was repeated at least twice. Typically, 100 mg of substrate, 50 mg of catalyst and 10 mL of H_2O were added to the reactor. Then, the sealed reactor was filled with hydrogen several times to remove air, and finally kept with 0.6 MPa of H_2. After that, the reactor was heated up to set temperature, and kept strring at 500 r/min. After completion of the reaction, the solid part was collected by centrifugation. The upper clear solution was passed through 0.22 um pore-size filter, and then analyzed by high performance liquid chromatography (HPLC) equipped with an Aminex HPX-87H® column (300 * 7.8 mm) and operated at 55 °C. The mobile phase was 0.5 M H_2SO_4 with a flow rate of 0.5 mL/min. The quantification of substrate conversion as well as product yield was calculated based on the external standard method, and the value of correlation coefficient (R^2) was above 0.999.

Glucose conversion and product yield were calculated by the following equations:

$$Glucose\ conversion\ (\%) = \frac{mole\ of\ converted\ glucose}{mole\ of\ initial\ glucose} \times 100\%$$

$$Yield\ of\ product\ (\%) = \frac{mole\ of\ generated\ product}{mole\ of\ initial\ glucose} \times 100\%$$

If lignocellulosic biomass was used as the substrate, its conversion was not measured, and the yield of product was calculated based on the following equation:

$$Yield\ of\ product\ (\%) = \frac{mole\ of\ generated\ product}{mole\ of\ glucose\ unit\ in\ initial\ lignocellulosic\ biomass} \times 100\%$$

Some other by-products including sorbitol, EG, PDO, lactic acid, and furan-

contained compounds were not individually quantified, and no gaseous product was generated by GC analysis.

Table S1 Textual properties of various samples (M = Mg, Zr, Al, Cr).

	Sample	SA[a] ($m^2\ g^{-1}$)	TPV[b] ($cm^3\ g^{-1}$)	Pd[c] (wt%)	Pd/W[c] (mol/mol)	M/W[c] (mol/mol)	Acidity[d] ($mmol\ g^{-1}$)
1	Pd-WO_x-MgO_y	57	0.14	2.3	0.05	0.12	1.5
2	Pd-WO_x-ZrO_y	265	0.17	1.7	0.05	0.53	1.4
3	Pd-WO_x-AlO_y	325	0.26	1.7	0.04	0.50	2.3
4	Pd-WO_x-CrO_y	186	0.11	1.8	0.05	0.48	2.5

[a] Surface area (SA) calculated in the relative pressure range of 0.001-0.1. [b] Total pore volume (TPV) at P/P_0=0.95. [c] Measured by ICP-OES. [d] Acidity of the prepared samples measured from NH_3-TPD analysis.

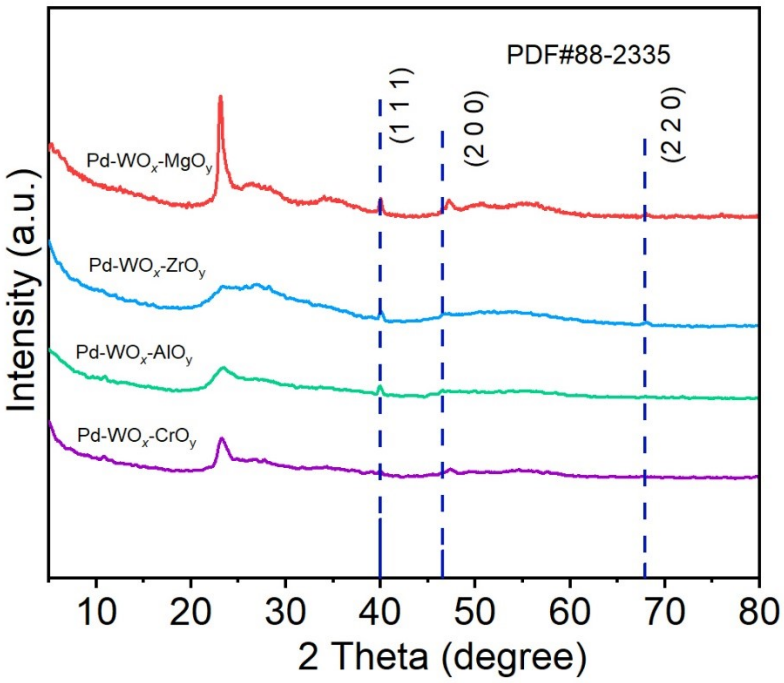

Fig. S1 XRD patterns of Pd-WO_x-MO_y (M = Mg Zr, Al, Cr) compared to the Pd standard PDF cards.

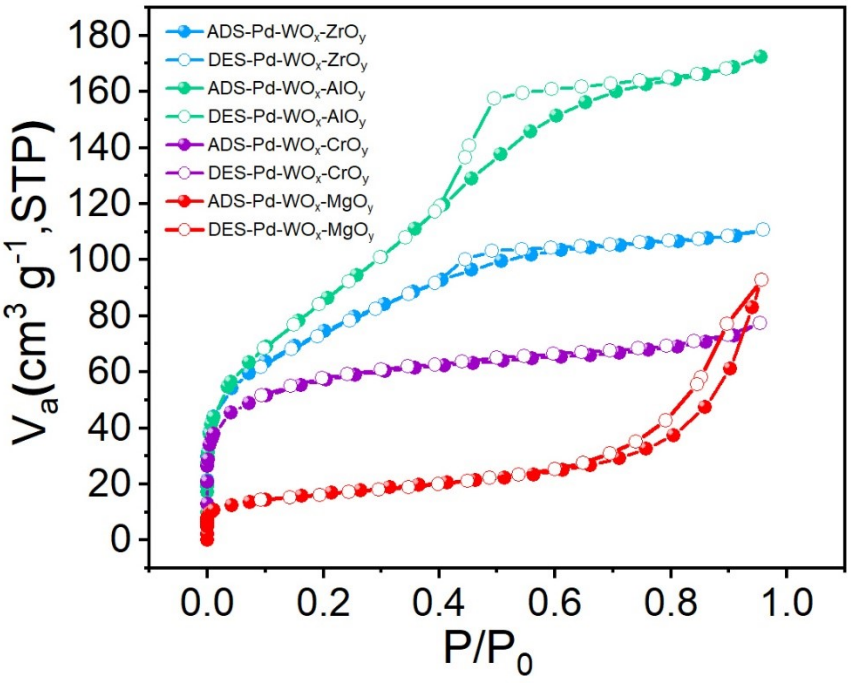

Fig. S2 N_2 adsorption-desorption isotherms of Pd-WO_x-MO_y (M = Mg, Zr, Al, Cr).

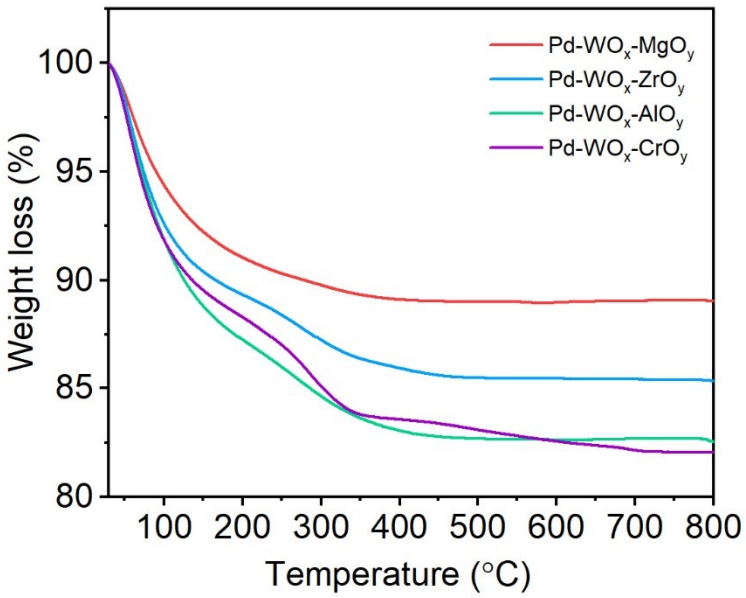

Fig. S3 TG curves of various sample.

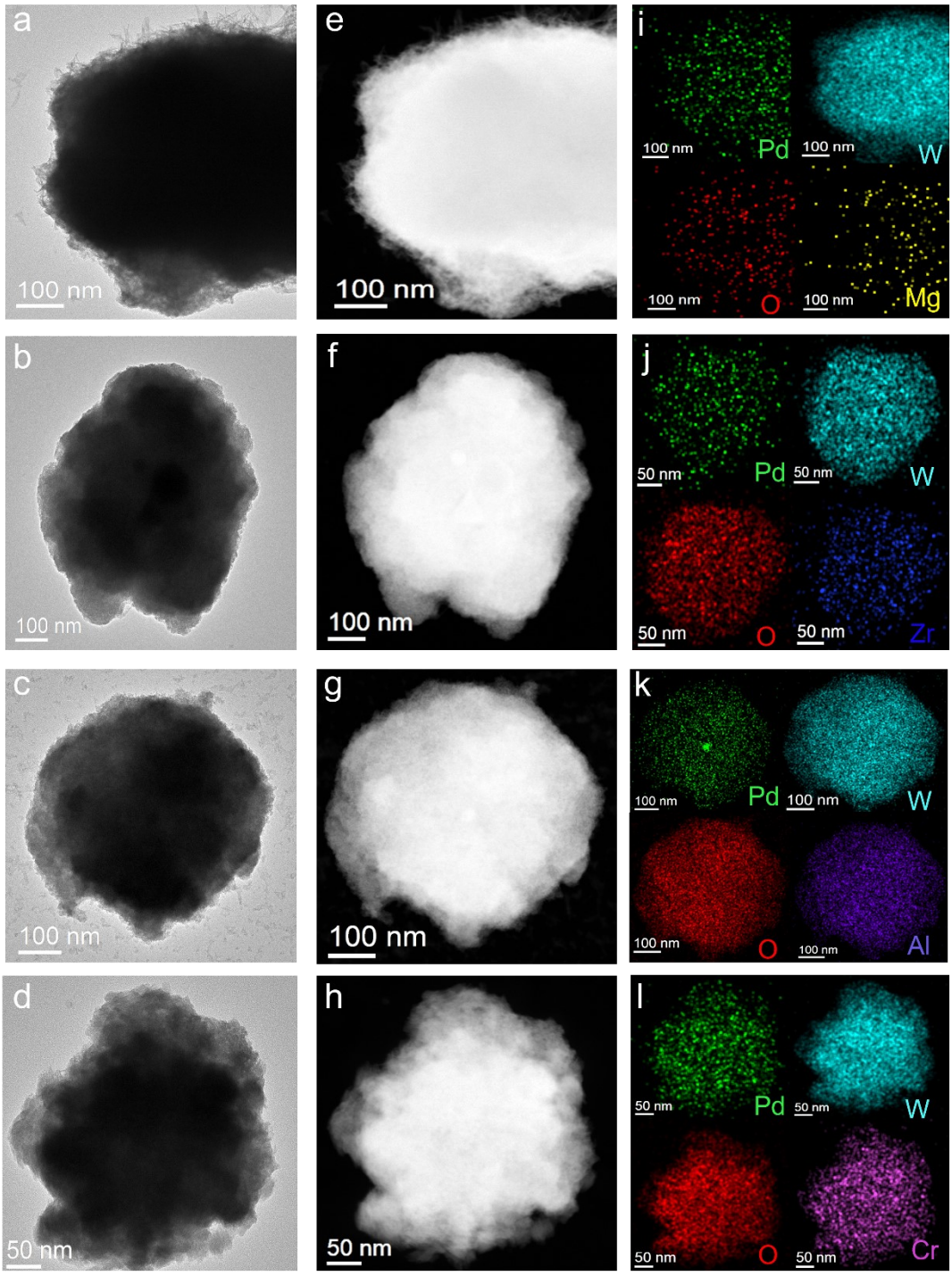

Fig. S4 TEM images (a-d), HAADF images (e-h), and EDS elemental mappings (i-l) of the corresponding Pd-WO_x-MgO_y, Pd-WO_x-ZrO_y, Pd-WO_x-AlO_y, and Pd-WO_x-CrO_y.

Table S2 The analytic results of O 1s XPS for Pd-WO_x-MO_y.[a]

Sample	Lattice oxygen (O_{lat})	Defective oxygen (O_{def})	Adsorbed oxygen (O_{ads})
Pd-WO_x-MgO_y	530.2	531.2	532.8
	23.1%	60.4%	16.5%
Pd-WO_x-ZrO_y	530.7	531.5	532.4
	49.9%	34.9%	15.2%
Pd-WO_x-AlO_y	530.6	531.4	532.4
	23.1%	20.3%	56.6%
Pd-WO_x-CrO_y	530.1	531.1	532.2
	21.2%	41.5%	37.3%

[a] Calculated based on its corresponding percentage in the deconvoluted XPS spectrum.

Table S3 The W 4f XPS analytic results of these four samples.[a]

Sample	W^{6+}(W $4f_{5/2}$)	W^{6+}(W $4f_{7/2}$)	W^{5+}(W $4f_{5/2}$)	W^{5+}(W $4f_{7/2}$)	W ($4f_{3/2}$)	W^{5+}/W^{6+}
Pd-WO_x-MgO_y	29.2%	26.6%	25.6%	13.4%	5.5%	0.70
Pd-WO_x-ZrO_y	28.0%	51.5%	8.1%	8.9%	3.5%	0.21
Pd-WO_x-AlO_y	37.8%	33.0%	9.5%	17.4%	2.5%	0.38
Pd-WO_x-CrO_y	30.5%	38.4%	12.2%	15.8%	3.1%	0.41

[a] Calculated based on its corresponding percentage in the deconvoluted XPS spectrum.

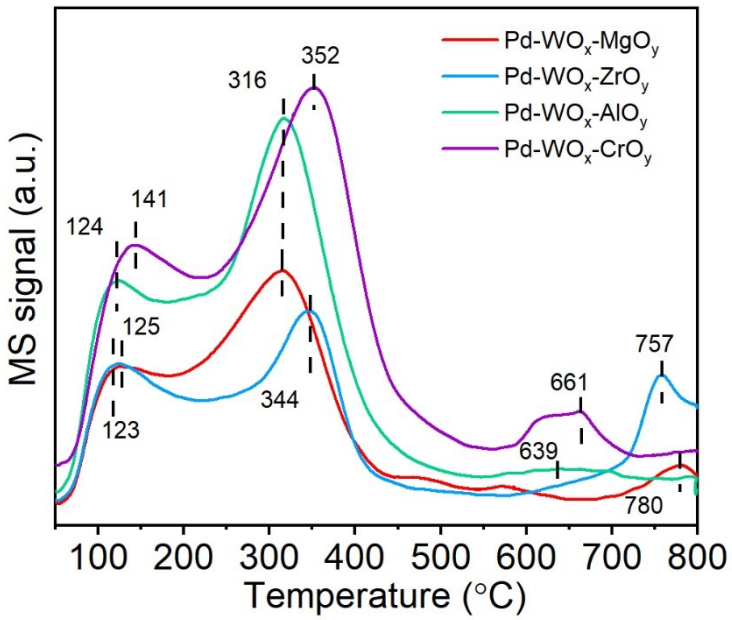

Fig. S5 NH_3-TPD curves of Pd-WO_x-MgO_y, Pd-WO_x-ZrO_y, Pd-WO_x-AlO_y, and Pd-WO_x-CrO_y.

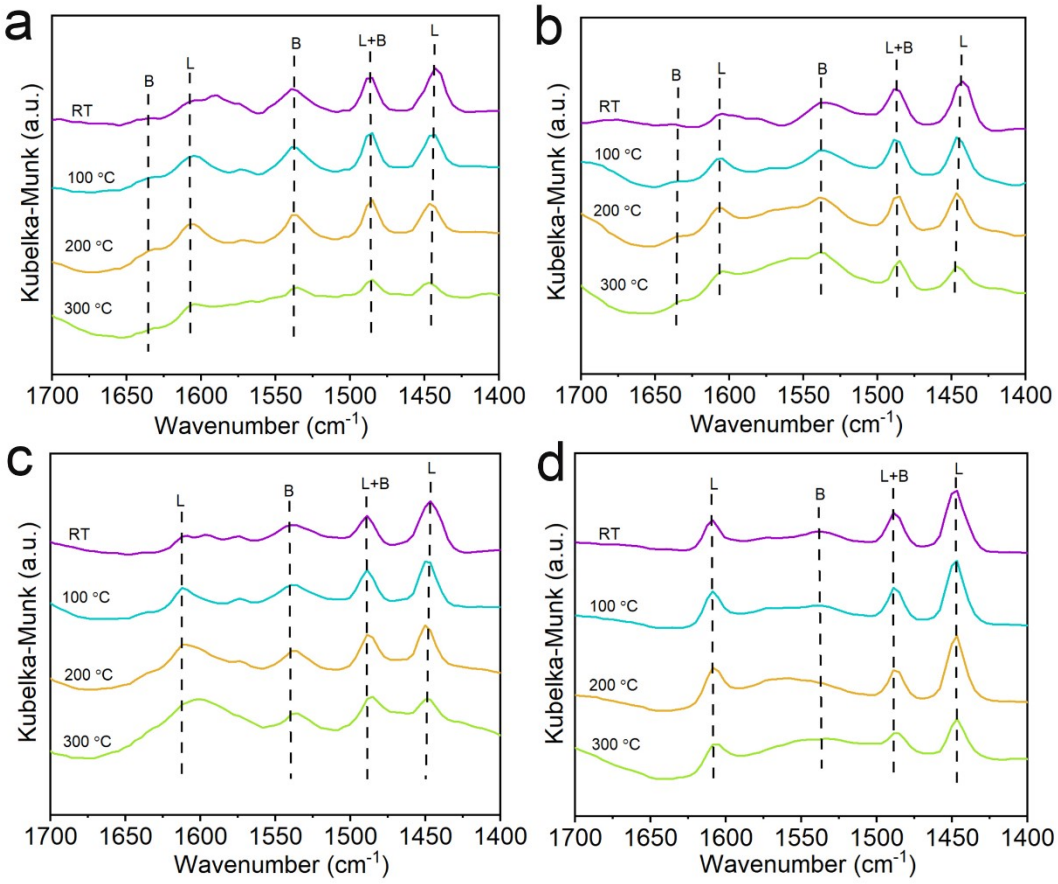

Fig. S6 Pyridine-adsorbed DRIFTS spectra of (a) Pd-WO_x-MgO_y, (b) Pd-WO_x-ZrO_y, (c) Pd-WO_x-AlO_y, and (d) Pd-WO_x-CrO_y. RT, L, and B represented room temperature, Lewis acid sites, and Brønsted acid sites, respectively.

Table S4 Quantitative analysis of acid sites from pyridine-adsorped DRIFTS performed at 100 °C.

Sample	Acid type		B/L
	L	B	
Pd-WO_x-MgO_y	5.8	6.0	1.03
Pd-WO_x-ZrO_y	3.4	2.4	0.70
Pd-WO_x-AlO_y	2.6	1.9	0.73
Pd-WO_x-CrO_y	5.3	2.1	0.39

Table S5 Comparison of various catalysts for the conversion of glucose to BDO.

Catalyst	T (°C)[a]	t (h)[b]	H_2 (MPa)	Conv. (%)	Yield (%) 1,2-BDO	Yield (%) 1,4-BDO	Reference
Pd-WO_x-MgO_y	160	4	0.6	>99	47.6	8.6	This work
10%Ce8%Cu/γ-Al_2O_3	200	6	4	100	10.2	\	[1]
Ni-Cu/4ZnO-CNT	245	6	5	100	6	\	[2]
Pt/SiO_2@$Mg(OH)_2$	180	4	6	>99	5	\	[3]
Ni-W/M	245	2	4	>99	<5	\	[4]

[a] T was short for reaction temperature. [b] t was short for reaction time.

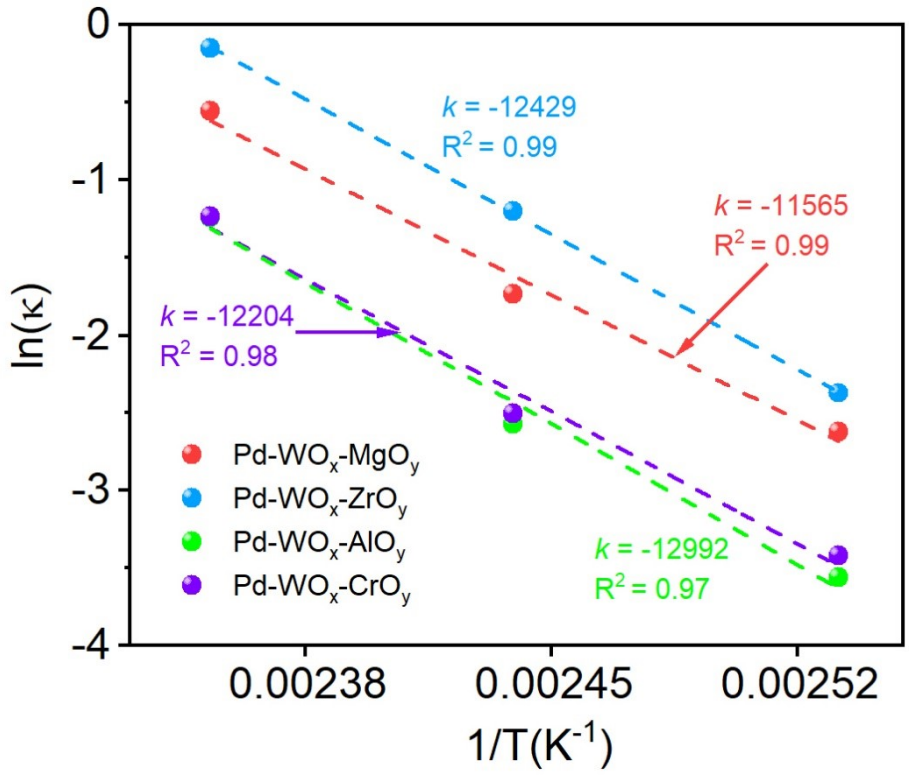

Fig. S7 The correlation between ln*k* and 1/T obtained from the kinetic analysis of (a) Pd-WO_x-MgO_y, (b) Pd-WO_x-ZrO_y, (c) Pd-WO_x-AlO_y, and (d) Pd-WO_x-CrO_y.

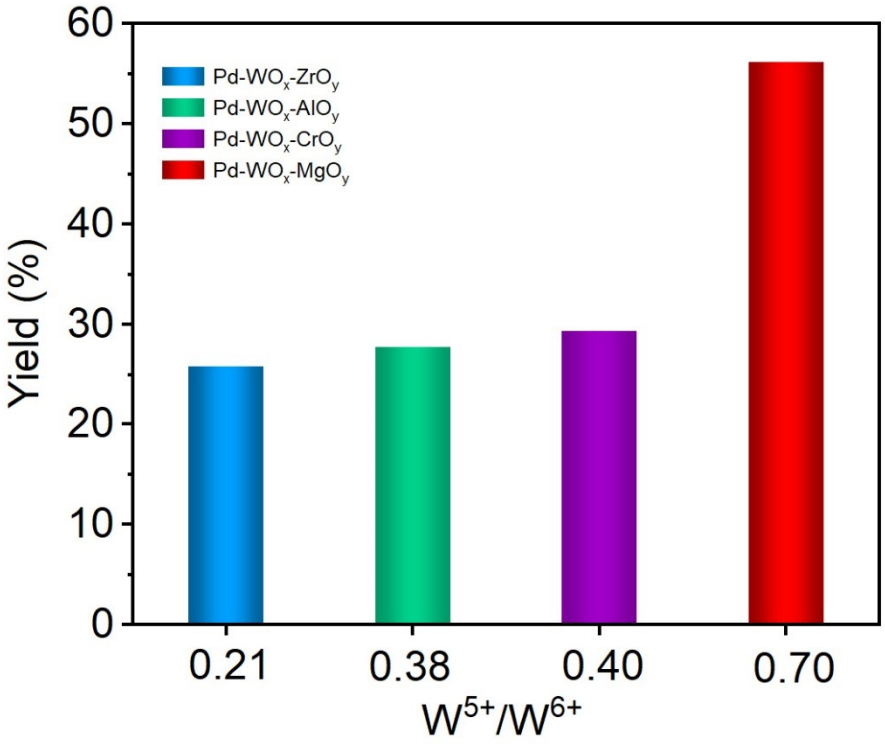

Fig. S8 Correlation between W^{5+}/W^{6+} ratio and BDO yield.

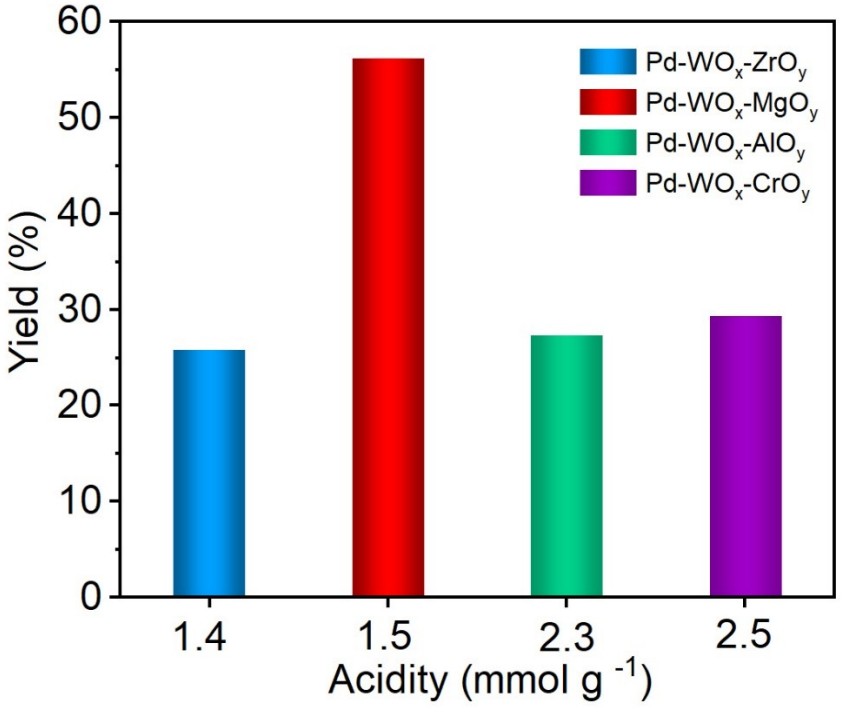

Fig. S9 Correlation between acidity and BDO yield.

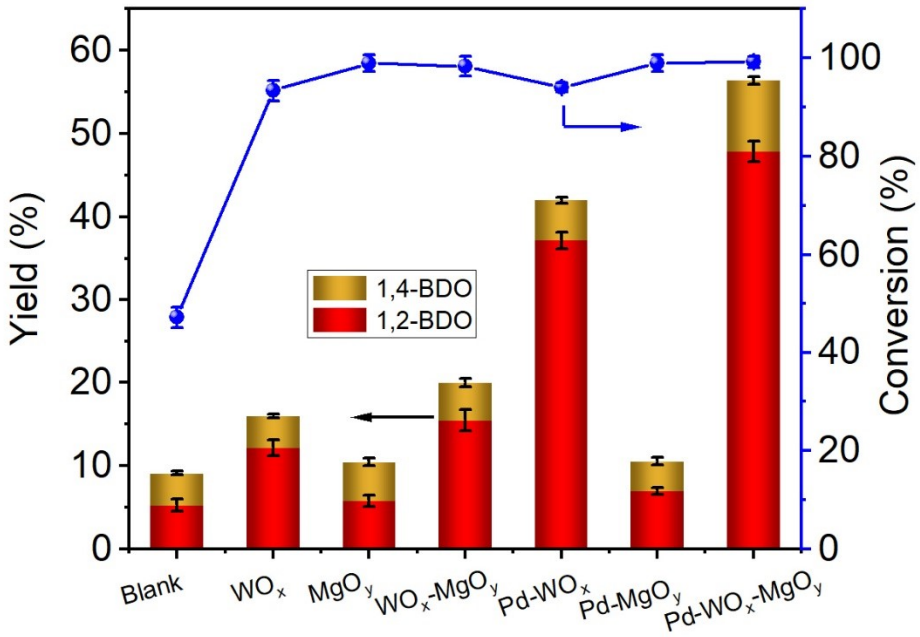

Fig. S10 Catalytic conversion of glucose to BDO over different catalysts. Reaction conditions:100 mg of glucose, 10 mL of water, 160 °C, 4 h, 0.6 MPa of H_2.

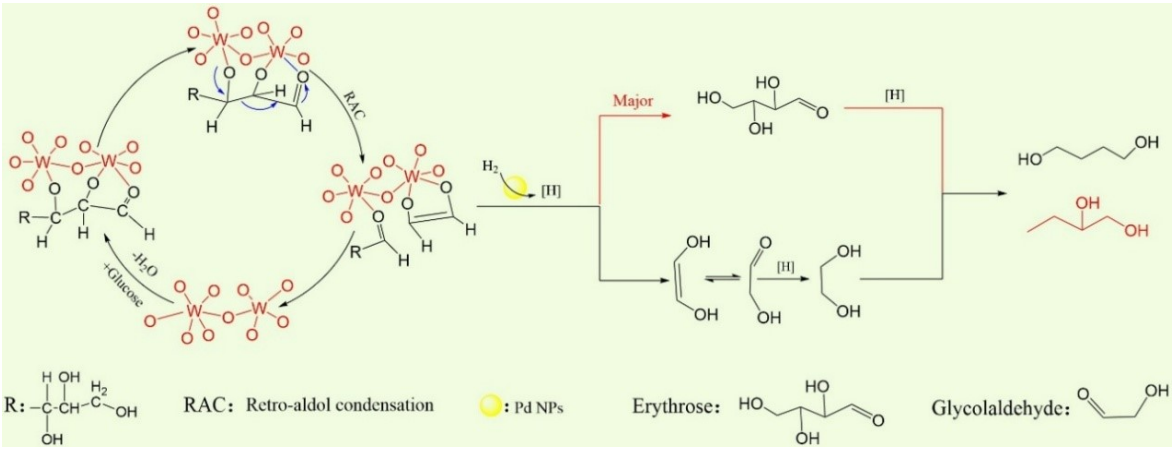

Fig. S11 Proposed reaction pathway for glucose conversion to BDO over Pd-WO_x-MgO_y.

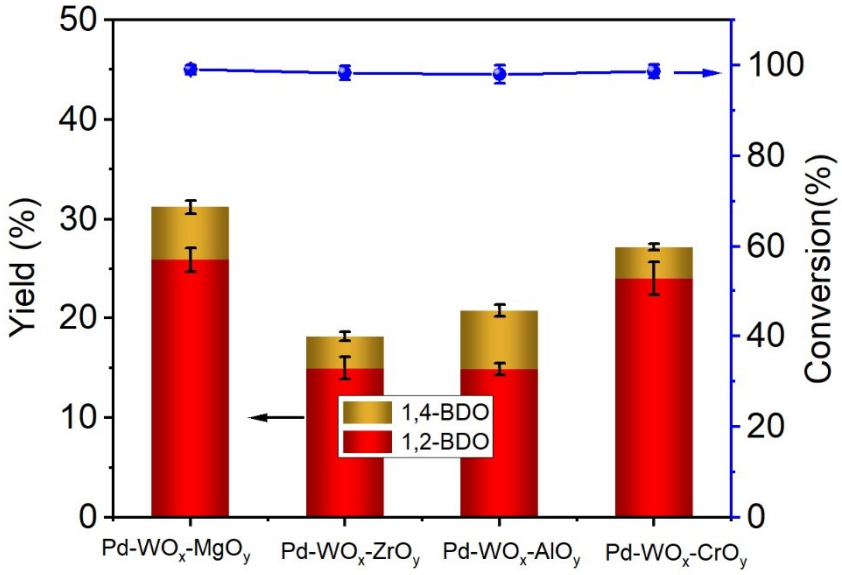

Fig. S12 Catalytic conversion of erythrose to BDO over Pd-WO_x-MO_y (M = Mg, Zr, Al, Cr). Reaction conditions: 100 mg of substrate, 10 mL of water, 160 °C, 4 h, 0.6 MPa of H_2.

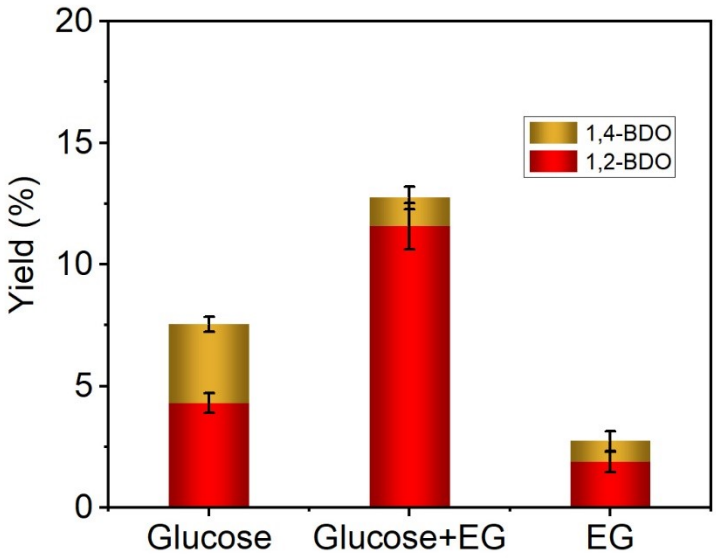

Fig. S13 Catalytic conversion of glucose and EG to BDO over Pd-WO_x-MgO_y. Reaction conditions: 100 mg of substrate, 10 mL of water, 160 °C, 4 h, 0.6 MPa N_2. Note: (Glucose+EG) represented 100 mg of glucose with extra 2 mL of EG.

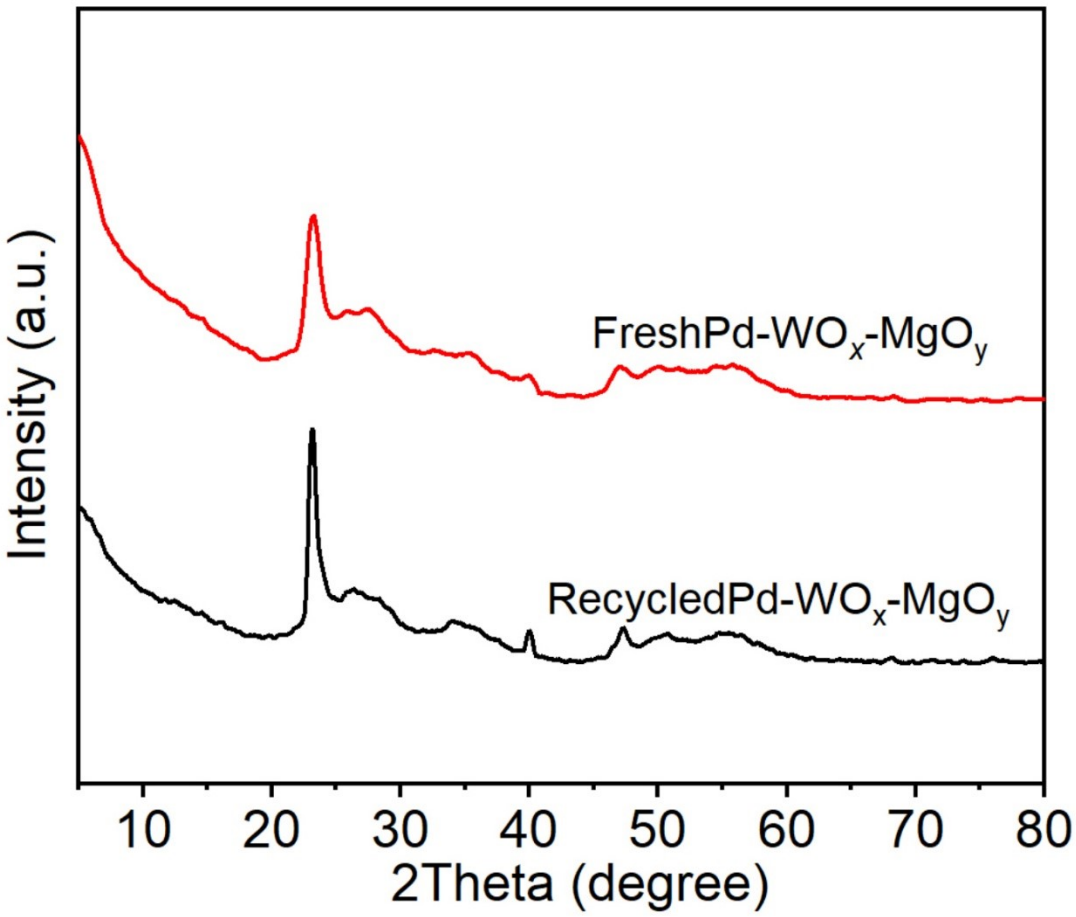

Fig. S14 XRD patterns of fresh and recycled Pd-WO_x-MgO_y.

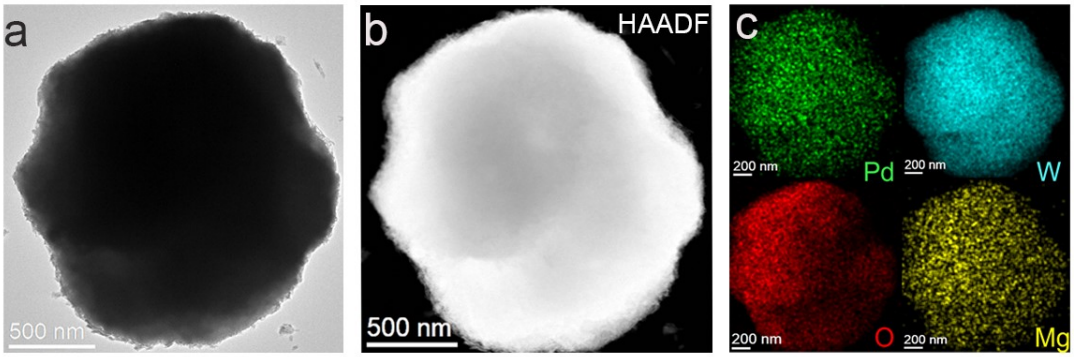

Fig. S15 (a) TEM image, (b) HAADF image, and (c) the mapping diagrams of the recycled Pd-WO_x-MgO_y.

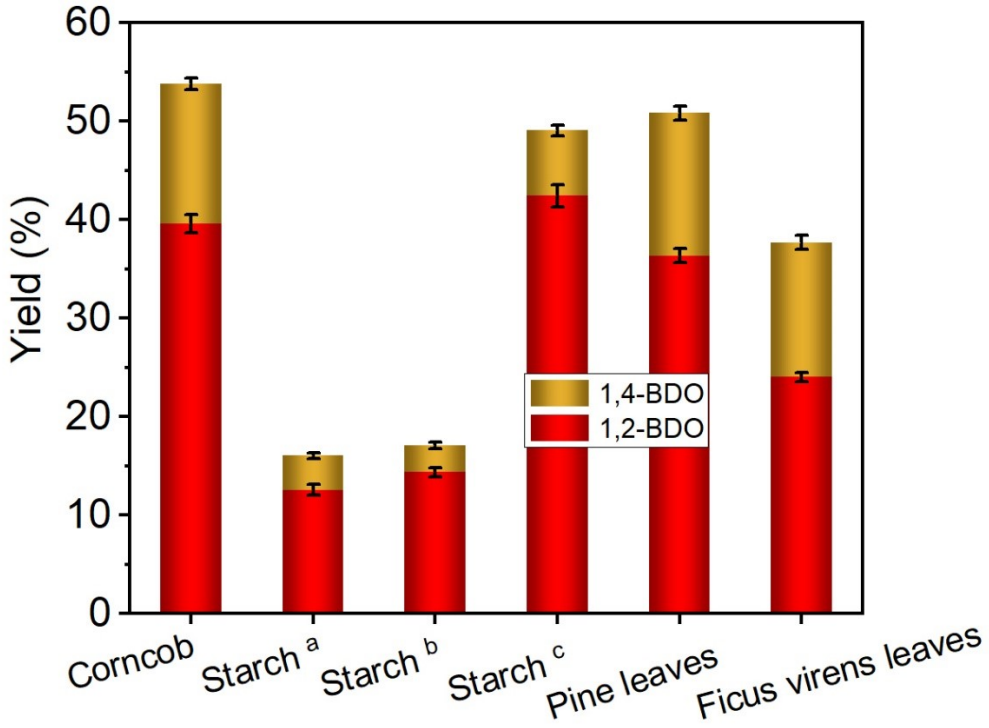

Fig. S16 Catalytic conversion of other substrates over Pd-WO_x-MgO_y.

Note: [a] Reaction conditions: 100 mg of substrate, 50 mg catalyst, 10 mL of water, 160 °C, 4 h, 0.6 MPa of H_2; [b] 100 mg of substrate, 100 mg catalyst, 10 mL of water, 160 °C, 4 h, 0.6 MPa of H_2; [c] 100 mg of substrate, 50 mg catalyst, 10 mL of water, 180 °C, 4 h, 0.6 MPa of H_2. The content of cellulose in Corncob, Pine leaves and Ficus virens leaves was 40 %, 25 % and 29 %, respectively.

References

[1] BALACHANDRAN KIRALI A A, SREEKANTAN S, MARIMUTHU B. Ce promoted Cu/γ-Al_2O_3 catalysts for the enhanced selectivity of 1,2-propanediol from catalytic hydrogenolysis of glucose [J]. Catalysis Communications, 2022, 165:106447.

[2] MA H, VAN DER WIJST C, MORKEN S F, et al. Directing the reaction pathway in the one-pot conversion of cellulose to vicinal diols by controlling bimetallic active sites in Ni-Cu/4ZnO-CNT catalysts [J]. Catalysis Today, 2024, 435:114709.

[3] GU M, SHEN Z, ZHANG W, et al. Hydrogenolysis of Glucose into Propylene Glycol over Pt/SiO_2@$Mg(OH)_2$ Catalyst [J]. ChemCatChem, 2020, 12(13): 3447-3452.

[4] LI N, LIU X, ZHOU J, et al. Enhanced Ni/W/Ti Catalyst Stability from Ti–O–W Linkage for Effective Conversion of Cellulose into Ethylene Glycol [J]. ACS Sustainable Chemistry & Engineering, 2020, 8(26): 9650-9659.